



HAL
open science

Lymphocyte radiosensitivity: An extension to the linear-quadratic model?

Thao-Nguyen Pham, Julie Coupey, Juliette Thariat, Samuel Valable

► To cite this version:

Thao-Nguyen Pham, Julie Coupey, Juliette Thariat, Samuel Valable. Lymphocyte radiosensitivity: An extension to the linear-quadratic model?. *Radiotherapy & Oncology*, 2024, 198, pp.110406. 10.1016/j.radonc.2024.110406 . hal-04624287

HAL Id: hal-04624287

<https://normandie-univ.hal.science/hal-04624287v1>

Submitted on 25 Jun 2024

HAL is a multi-disciplinary open access archive for the deposit and dissemination of scientific research documents, whether they are published or not. The documents may come from teaching and research institutions in France or abroad, or from public or private research centers.

L'archive ouverte pluridisciplinaire **HAL**, est destinée au dépôt et à la diffusion de documents scientifiques de niveau recherche, publiés ou non, émanant des établissements d'enseignement et de recherche français ou étrangers, des laboratoires publics ou privés.

Journal Pre-proofs

Original Article

Lymphocyte radiosensitivity: An extension to the linear-quadratic model?

Thao-Nguyen Pham, Julie Coupey, Juliette Thariat, Samuel Valable

PII: S0167-8140(24)00676-5

DOI: <https://doi.org/10.1016/j.radonc.2024.110406>

Reference: RADION 110406

To appear in: *Radiotherapy and Oncology*

Received Date: 6 March 2024

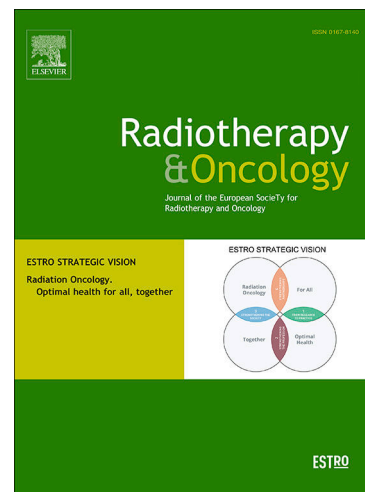
Revised Date: 13 June 2024

Accepted Date: 17 June 2024

Please cite this article as: Pham, T-N., Coupey, J., Thariat, J., Valable, S., Lymphocyte radiosensitivity: An extension to the linear-quadratic model?, *Radiotherapy and Oncology* (2024), doi: <https://doi.org/10.1016/j.radonc.2024.110406>

This is a PDF file of an article that has undergone enhancements after acceptance, such as the addition of a cover page and metadata, and formatting for readability, but it is not yet the definitive version of record. This version will undergo additional copyediting, typesetting and review before it is published in its final form, but we are providing this version to give early visibility of the article. Please note that, during the production process, errors may be discovered which could affect the content, and all legal disclaimers that apply to the journal pertain.

© 2024 Elsevier B.V. All rights are reserved, including those for text and data mining, AI training, and similar technologies.



Lymphocyte radiosensitivity: an extension to the linear-quadratic model?

Thao-Nguyen Pham^{1,2}, Julie Coupey¹, Juliette Thariat^{2,3*}, Samuel Valable^{1*}

¹Université de Caen Normandie, CNRS, Normandie Université, ISTCT UMR6030, GIP CYCERON, F-14000 Caen, France

²Laboratoire de physique corpusculaire UMR6534 IN2P3/ENSICAEN, France - Normandie Université, France

³Department of Radiation Oncology, Centre François Baclesse, Caen, Normandy, France

*Authors equally contributed/Corresponding authors

Corresponding authors

Samuel VALABLE, ISTCT UMR6030, Boulevard Henri Becquerel, GIP CYCERON, 14000 Caen, France
samuel.valable@cnrs.fr

Juliette THARIAT, LPC Caen ENSICAEN UMR6534, 6 Boulevard Maréchal Juin, 14050 Caen, France
jthariat@gmail.com

Running title: A saturation model for lymphocyte radiosensitivity

Highlights

- The linear-quadratic model, commonly used to analyze the impact of radiation on cells, has shown restrictions when applied to lymphocytes.
- Our research presents the saturation model, which considers a negative exponential relationship between radiation dose and cell response to radiation, addressing potential non-linear responses of lymphocytes to radiation.
- The saturation model offers a more accurate representation of lymphocyte response to radiation.
- The saturation model can be used to assess T lymphocyte survival following exposure to X-ray and proton irradiation and observe time dependencies.

Abstract

Background and purpose: The linear-quadratic (LQ) model has been pivotal for evaluating the effects of radiation on cells, but it is primarily characterized by linear responses, which has exhibited limitations when applied to lymphocyte data. The present research aims to address these limitations and to explore an alternative model extended from the conventional LQ model.

Materials and methods: literature providing lymphocyte counts from assays investigating apoptosis and survival after *in vitro* irradiation was selected. To address the nonlinearity in lymphocyte responses to radiation, we developed a saturation model characterized by a negative exponential relationship between radiation dose and cellular response. We compared the performance of this saturation model against that of conventional models, including the LQ model and its variants (linear model LM and linear-quadratic-cubic model LQC), as well as the repair-misrepair (RMR) model. The models were evaluated based on prediction-residual plots, residual standard errors, and the Akaike information criterion (AIC). We applied the saturation model to two additional datasets: (1) a dataset from the existing literature that assessed stimulated and unstimulated human lymphocytes exposed to gamma irradiation *in vitro* and (2) a novel dataset involving T lymphocytes from rodent spleens after exposure to various radiation types (X-rays and protons).

Results: The literature (n=15 out of 2342) showed that lymphocyte apoptosis varies with dose, time and experimental conditions. The saturation model had a lower AIC of 718 compared to the LM, LQ, LQC and RMR models (AIC of 728, 720, 720 and 734, respectively). The saturation model had a lower residual error and more consistent error distribution. Integrating time as a covariate, the saturation model also had a better AIC for demonstrating time-dependent variations in lymphocyte responses after irradiation. For datasets involving unstimulated lymphocytes before irradiation, the saturation model provided a more accurate fit than did the LM, LQ, and RMR models. In these cases, the fit of the saturation model was comparable to that of the LQC model but offered an advantage when extrapolating to higher doses, where the LQC model might underestimate survival. For stimulated lymphocytes, which are radioresistant, all the models approximated the LM. Both the LQ and saturation models indicated greater radiosensitivity to protons *in vitro*.

Conclusion: The new “saturation model” performed better than the LQ model in quantifying lymphocyte apoptosis and survival, estimating time dependency and assessing the role of radiation modalities or lymphocyte stimulation. Further experiments are warranted to experimentally explore the validity of the saturation model as a promising alternative in the clinical setting.

Keywords: lymphocyte, radiosensitivity, linear-quadratic model, radiation dose–response

Lymphocyte radiosensitivity: a substitution model to the linear-quadratic model?

A saturation model for lymphocyte radiosensitivity

1 Introduction

Beyond its effectiveness in controlling tumor growth, radiotherapy can result in weakening of the body's immune system by causing radiation-induced lymphopenia (RIL). RIL occurs in miscellaneous cancer types in patients [1,2]. One of the hypotheses underlying RIL is the high radiosensitivity of lymphocytes exposed to radiation doses during radiotherapy. Following this hypothesis, several studies have aimed to model the effects of direct lymphocyte exposure to radiation by 1) modeling the dose that each lymphocyte receives during irradiation and 2) modeling the dose effect on lymphocytes (i.e., lymphocyte radiosensitivity). In addition, the radiation-induced lymphocyte apoptosis assay (RILA) has recently emerged as a potential predictor for radiation-induced normal tissue complications in various types of solid cancers, such as breast cancer [2–6]. However, correlations between RILA and outcomes are not fully consistent across studies [6] and with previous modeling studies using the most common radiosensitivity model, i.e., the linear-quadratic (LQ) model. Therefore, better prediction of lymphocyte radiosensitivity may be needed to understand clinical outcomes.

The LQ model dates back to 1962 when Douglas Lea initially fitted the average yield of chromosomal aberrations per cell in the form of an LQ relationship with a single dose [7]. Since then, theoretical approaches at different physical and biological scales, such as molecular damage reparability and lethal chromosomal aberration yields in tumor and normal tissue cells, all approximate the LQ formulation [8]. The LQ model showed good agreement with experimental data over the ranges typically used in colony formation assays [9].

Beyond the LQ model, there are numerous variants and other mechanistic-based models tailored specifically for different cancer cell lineages. Within the realm of lymphocytes, however, the LQ model without the quadratic component (i.e., the linear model, LM) has gained prominence for *in vitro* prediction of lymphocyte survival under irradiation. The better performance of the LM over the LQ model was considered due to the high radiosensitivity of lymphocytes, and the double-hit effect of the quadratic component was not needed [10,11]. In addition, the LQ model is also more effective for tissues that repopulate slowly, such as those in the central nervous system (e.g., brain and spinal cord) [12]. However, this is not the case for lymphocytes. Lymphocyte repopulation can be accelerated when irradiation is below a certain threshold [13]. Consequently, a high repopulation rate of surviving lymphocytes after radiation exposure may align better with the linear model.

In addition, with advancements in biological assays, more assays beyond colony survival assays have been employed to investigate more mechanistic aspects of lymphocyte radiosensitivity. One major mechanism of lymphocyte cell death is apoptosis [6], and other assays, such as the Annexin V assay for cell apoptosis or the RILA assay for lymphocyte apoptosis, are being used. When the LQ model was applied to fit multiple *in vitro* datasets, the resulting curve failed to accurately represent the data, particularly when alternative assays were used instead of the colony survival assay [14].

Under these considerations, we develop a new model, the saturation model, in an attempt to outperform the LQ model. We further investigated the time dependency and differences in lymphocyte survival under exposure to X-ray or proton irradiation using LQ and saturation models.

2 Materials and methods

2.1 Literature search of published data on lymphocyte apoptosis following irradiation *in vitro*

Lymphocyte apoptosis following irradiation *in vitro* data were collected by searching the PubMed database using the search terms “lymphocyte radiosensitivity *in vitro*” or “radiation-induced lymphocyte apoptosis” from 1980 to 2023. The data were digitally extracted using PlotDigitizer [15]. The data were stratified according to the endpoint (cell survival, apoptosis/non-apoptosis fractions), lymphocyte type and assay used for radiosensitivity.

2.2 Lymphocyte radiosensitivity model

2.2.1 Linear-quadratic model and its variants

Since the early stages of radiobiological research, the LQ has been viewed primarily as an empirical fitting model to represent dose-effect relationships [7]. The widespread applicability of LQ models to radiosensitivity data has led to several biological interpretations supporting their relevance [16]. Among these interpretations, one of the most prominent is based on the hit theory [9]. The LQ model assumed (eq. 1) a linear relationship between dose and non-repairable damage and radiation dose; (2) a quadratic relationship between dose and repairable DNA damage and radiation dose; and (3) a Poisson distribution of cell survival over DNA damage.

$$SF = \exp(-\alpha D - \beta D^2) \text{ (eq.1)}$$

where $SF(\%)$ is the fraction of surviving cells, D is the radiation dose (Gy), α (Gy^{-1}) represents the lethal damage caused by a single incident particle (unrepaired damage), and β (Gy^{-2}) represents 'multiple hit' cell death (damage from different radiation tracks) [9].

In 1990, Nakamura and colleagues conducted an *in vitro* investigation to assess the radiosensitivity of proliferating lymphocytes using a colony formation assay [17]. In their study, the observed cell survival curves conformed to a linear-quadratic dose-response pattern, as determined by the linear quadratic model with $\alpha=0.29\pm0.01$ (Gy^{-1}) and $\beta=0.14\pm0.01$ (Gy^{-2}).

Notably, however, the response curves in the majority of the *in vitro* studies examined typically exhibit either an exponential or upward-sloping trend with a saturation in response at higher doses when some assay other than the colony formation assay is applied [14]. This suggests that (1) lymphocytes are a very radiosensitive cell line with lethal unrepaired DNA damage. (2) The relationship between non-repairable damage and radiation dose is linear when the dose is low and is saturated when the dose is high. A substitution for the LQ model could be the linear dose-response model (so-called linear model, eq. 2), where only lethal DNA damage is accounted for and sublethal DNA damage is neglected (β fixed as 0).

$$SF = \exp(-\alpha D) \text{ (eq.2)}$$

Furthermore, the LQ model describes the cellular response to ionizing radiation extremely well at doses less than 5–6 Gy and is the preferred model for this dose range [18]. Some observations have indeed shown that at higher doses, the survival response of cells is often found to more closely resemble a linear relationship between $-\log(\text{survival fraction})$ and dose [18]. Thus, at a higher dose range, modifications to the original LQ model include adding a term proportional to the cube of the dose but with an opposite sign to the linear and quadratic terms, creating the linear-quadratic-cubic (LQC) model (eq. 3) [16,18].

$$SF = \exp(-\alpha D - \beta D^2 + \gamma D^3) \text{ (eq.3)}$$

2.2.2 Repair-misrepair model

The repair-misrepair (RMR) model, one of the earliest mechanistic-based radiosensitivity models, is based on the sublesion hypothesis [16,19], in which the production of DNA lesions and subsequent expression of biological effects are distinctly different phases of the entire process [19]. The function $U(t)$, proposed by Tobias in 1985 [19], reflects the mean number of lesions before any repair activation.

$$SF = \exp(-\delta D) \left(1 + \frac{\delta D}{\epsilon}\right)^\epsilon \text{ (eq.4)}$$

where $SF(\%)$ is the fraction of surviving cells, D (Gy) is the irradiation dose, δ (Gy^{-1}) is the proportion between the initially induced lesions and radiation dose, and ϵ is the relative repair ratio between self-repair and misrepair.

2.2.3 Saturation model

We derived a new model from the current linear-quadratic model. Similar to the mechanistic inference of the linear-quadratic model, we assumed a Poisson distribution of cell survival over DNA damage.

$$SF = \exp(-DNA \text{ damage})$$

where $SF(\%)$ is the fraction of surviving cells. Then, we assumed a negative exponential relationship between the dose and DNA damage.

$$DNA \text{ damage} = DNA \text{ damage}_{sat} * (1 - e^{-\mu D})$$

where D is the radiation dose in Gy. $DNA \text{ damage}_{sat}$ is the maximum proportion of DNA damage when the dose is high ($D \rightarrow +\infty$) and is independent of the dose D . μ (Gy^{-1}) is the increase in the rate of DNA damage when the dose D increases. The minimum survival rate at a high dose ($D \rightarrow +\infty$) corresponding to the maximum proportion of DNA damage (SF_{sat}) was calculated as

$$SF_{sat} = \exp(-DNA \text{ damage}_{sat}) \Leftrightarrow DNA \text{ damage}_{sat} = -\log(SF_{sat})$$

Since $SF_{sat} \leq 1$, $\log(SF_{sat}) \leq 0$. The new surviving fraction estimate becomes:

$$SF = \exp(-DNA \text{ damage}_{sat} * (1 - e^{-\mu D})) = \exp(\log(SF_{sat}) * (1 - e^{-\mu D})) \quad (eq.5)$$

where $SF(\%)$ is the fraction of surviving cells and $SF_{sat}(\%)$ is the value SF at which SF is stable and stops increasing with increasing dose D (Gy). Since μ (Gy^{-1}) signifies the rate of increase in DNA damage as the dose increases, a higher μ value means that $SF(\%)$ reaches $SF_{sat}(\%)$ at a lower radiation dose (Supplementary section 1, Figure S1). At low doses ($D \rightarrow 0$), the saturation model approximates the linear model with $\log\left(\frac{1}{SF_{sat}}\right) * \mu$ (Gy^{-1}) (see supplementary section 2).

For model evaluation, we included only data analyzing total peripheral lymphocyte radiosensitivity and used Annexin V to quantify lymphocyte apoptosis.

2.3 Model performance comparison

The performance of the saturation model was compared with that of other radiosensitivity models. Data from human peripheral blood lymphocytes undergoing apoptosis (i.e., Annexin V positive) were selected for model development from the literature (N=15 publications).

2.4 Model application

2.4.1 Example 1: Comparison of the radiosensitivity of lymphocytes irradiated after stimulation with CD3/CD28 antibodies or without stimulation

We applied the saturation model to a dataset from Heylmann *et al.* 2018 [20] of either stimulated or unstimulated peripheral blood lymphocytes (PBLs), helper T lymphocytes (Ths), and cytotoxic T lymphocytes (CTLs) extracted from healthy donors. Cells were either stimulated or not with CD3/CD28 antibodies within 48 hours. One hour following stimulation, the cells were exposed to γ -irradiation at doses ranging from 0.125 to 2 Gy. Apoptotic cells were quantified using an Annexin V assay at 12 hours post-irradiation (details in [20]). Data on the fraction of cells undergoing apoptosis were extracted using PlotDigitizer [21].

2.4.2 Example 2: Comparing lymphocyte radiosensitivity following X-ray or proton irradiation

We applied the saturation model in our experimental dataset of T-CD8+ lymphocyte survival following exposure to X-ray or proton irradiation to explore its potential impact on radiosensitivity. T-CD3+ lymphocytes were

extracted from the spleens of healthy Swiss mice. An EasySep™ Mouse T-Cell Isolation Kit (19851, StemCell) was used to isolate lymphocytes from single-cell splenocyte suspensions by negative selection.

Undesired cells were separated using an EasySep™ magnet (18000, StemCell), and lymphocytes were seeded in 24-well plates pre-coated with 1 µg/mL of anti-CD3ε (100340, Biolegend) in RPMI medium supplemented with 20 U/mL of IL-2 (21212, PeproTech), and 1 µg/mL of anti-CD28 (102116, Biolegend) was added to the isolated lymphocyte suspension before seeding at 1 mL/well.

After 48 hours of culture, cells were irradiated with either X-rays (FAXITRON, Cyceron, Caen, France) or protons (from an IBA ProteusOne at the Normandy Proton Therapy Center CYCLHAD, Caen, France) at 0.5, 1, 2 or 4 Gy. X-ray exposure was performed at 2 Gy/min (130 keV/5 mA/Cu filter). For protons, the LET was calculated to be 4.6 keV/µm.

After irradiation, the cells were incubated for 24, 48, or 72 hours before cell counting. The fraction of surviving cells was calculated in percentage. The whole dataset of X-ray- and proton-irradiated cells was fitted with the saturation model considering time after irradiation (eq. 6). The SF_{sat} parameter was estimated separately for the X-ray and proton data. The surviving fraction at 2 Gy (SF2) of lymphocytes undergoing X-ray or proton irradiation was then calculated from the model.

2.5 Statistical methods

Fitting of the model parameters was performed using the nlme package version 3.1-160 [22,23] with RStudio version 4.1.2 [24]. Model performance was first evaluated by plotting the prediction versus residual values. A better model resulted in a less or insignificant correlation between the predicted and residual values. The likelihood ratio test was used to assess the significance of differences in model performance between different models. A better model fit was defined by a lower residual standard error (RSE, calculated with respect to the survival fraction) and Akaike information criterion (AIC).

3 Results

Fifteen publications were identified [17,20,25–37], of which six analyzed total peripheral lymphocytes and others analyzed lymphocyte subtypes (supplementary section 3, Table S1). The literature selection flowchart is illustrated in Figure 1 (see supplementary section 3, Table S2 for details of the selected studies). Of the five Annexin V assay publications [25,26,28,29,31], one analyzed the impact of dose rate on bovine lymphocyte survival *in vitro*. There was a decreasing trend in the non-apoptotic lymphocyte fraction as both dose and time increased, with saturation starting at 5 Gy or extended times of ≥ 48 hours following irradiation (Figure 2A, B). Regarding the dose rate effect, a low dose rate induced a decrease in bovine lymphocyte survival *in vitro* [38]. It was suggested that the inverse effect of the dose rate on lymphocyte survival occurred immediately after irradiation, suggesting interphase death by membrane damage rather than cell killing by DNA damage [38]. There was considerable cell loss at a low dose rate, which was negligible when the dose rate increased to higher than 0.3 Gy/min (Figure 2C). The dose effect on lymphocytes at a very small dose (0.006 Gy/min) followed LQ function (Figure 2D). However, a small dose rate of ≤ 0.3 Gy/min is not relevant to clinical external beam radiotherapy. Therefore, the effect of the dose on the lymphocyte radiosensitivity model was considered negligible.

Next, we compared the performance of the LM, LQ, LQC, and saturation models based on lymphocyte apoptosis data from post-irradiation Annexin V assays using photon beams at a minimum of 0.5 Gy/min. Our analysis revealed significantly different performances between the models (supplementary section 4, Table S3). The linear model displayed a correlation between the residual error and the predicted value ($p = 0.02$) (Figure 3B.1). In contrast, the LQ, LQC, and saturation models exhibited no correlation between the residual error and the predicted value ($p > 0.1$, as detailed in Figures 3B.2, 3, and 4), indicating a better fit to the data compared to the LM. Parameter estimation for both the LQ and LQC models yielded negative values for parameters β and γ , contradicting the expected positive values based on the models' theoretical frameworks. The saturation model returned a lower residual error and AIC ($p < 0.05$ using Fisher's exact test) compared to the linear, LQ, and LQC models (supplementary section 4, Table S3). Such better performances were also observed when the data were fitted separately for each study (lower residual error and AIC, $p < 0.05$ using Fisher's exact test; see supplementary section 5, figures S2-S5, tables S4-S7).

We then compared the saturation model fitting with either common SF_{sat} or separated SF_{sat} models for each time after irradiation. The saturation model with a separated SF_{sat} for each incubation time after irradiation resulted in better performance compared to one with a common SF_{sat} estimation (lower residual error and AIC, $p < 0.05$ using Fisher's exact test; Figure 4; for details, see supplementary section 6, Table S8). In the saturation model with separated SF_{sat} for each time after irradiation, SF_{sat} had a positive correlation with the post-irradiation time (Figure 4C).

We introduced the effect of time after irradiation in the saturation model.

$$SF = \exp(\log(SF_{sat}) * (1 - e^{-\mu D})) \text{ with } SF_{sat} = 1 - kt \text{ (eq. 6)}$$

where t is the time after irradiation in hours.

A difference in model performance between the saturation model without or with time effects was detected (Table 1D, G, $p < 0.05$ using Fisher's exact test). Considering the effect of incubation time after irradiation on SF_{sat} , the model returned a lower RSE and AIC with better residual distribution (Figure 4A). The saturation and conventional LM incorporating time effects were compared (eq. 7).

$$SF = \exp(-\alpha D) \text{ with } \alpha = 1 - kt \text{ (eq.7)}$$

where t is the time after irradiation in hours.

When incorporating time into the model, the saturation model outperformed the LM (lower residual standard error and AIC, supplementary section 7, Table S9), and there was no correlation between RSE and PV in the saturation model ($p > 0.1$, Figure 5A.1) versus a significant correlation in the LM ($p < 0.05$, Figure 5A.2). In addition, there was no significant change in parameter estimates and better model performance when data uncertainty was considered (further details are provided in supplementary section 8, figure S6, and table S10).

We subsequently compared the performance of the linear and saturation models using a restricted dataset where the dose did not exceed 5 Gy. The performances were similar (Table 5, $p > 0.05$ under Fisher's exact test). This similar performance was expected as the LM is mathematically contained as a special case in the SM (see supplementary section 2). Additionally, neither model showed a correlation between the residuals and the predicted values (Figure 5B).

To illustrate the utility of the saturation model, we applied the saturation model to two scenarios. First, we utilized the dataset from Heylmann *et al.* 2018 [20] of either stimulated or unstimulated peripheral blood lymphocytes (PBLs), helper T lymphocytes (Ths), and cytotoxic T lymphocytes (CTLs) extracted from healthy donors. For the unstimulated PBLs, Ths, and CTLs, the saturation and linear-quadratic-cubic models achieved better fits than did the linear-quadratic and repair-misrepair models (Figure 6A, lower AIC values, $p < 0.01$, according to Fisher's exact test; see supplementary section 9, Tables S11-15). Upon stimulation with a CD3/CD28 antibody, PBLs, Ths, and CTLs exhibited increased radioresistance compared to that of the unstimulated population. For stimulated PBL, Th, and CTL, all the models, including linear, linear-quadratic, linear-quadratic-cubic, repair-misrepair, and saturation models, yielded similar results (Figure 6A, see supplementary section 9, tables S11-15 for parameter estimation).

According to the saturation model, the survival fractions at 2 Gy (SF2) for stimulated PBL, Th, and CTL were 84.5%, 84.6%, and 87.1%, respectively. In contrast, SF2 for the unstimulated populations was significantly lower: 55.6% for PBL, 46.6% for Th, and 53.2% for CTL. The SF_{sat} for stimulated PBL, Th, and CTL was found to be 84.1%, 84.7%, and 87.1%, respectively, while for the unstimulated groups, they were 54.7% for PBL, 46.5% for Th, and 53.2% for CTL. These SF2 values approached the corresponding lowest survival rates (SF_{sat}) for each population, i.e., a dose of 2 Gy was sufficient for these lymphocyte populations to reach their saturated survival value.

Second, we utilized our own experimental dataset of T-CD8+ lymphocyte survival following exposure to X-ray or proton irradiation. The reduction rate of SF_{sat} with time for both the X-ray and proton data was better estimated with the saturation model than with the linear model ($p < 0.01$ for likelihood ratio test). Parameter estimates for each radiation type separately showed a greater rate of decrease in the saturated steady-state level over time

with protons compared to X-rays (for a higher value of k , see supplementary section 10, Table S16). Model fitting of dose–survival curves indicated that rodent splenic T-CD8+ lymphocytes were more sensitive to X-rays than to protons (Figure 6A). The SF2 of lymphocytes subjected to X-rays was 86.84%, 73.05% and 58.41% at 24, 48 and 72 hours post-irradiation, respectively. These values were higher than those observed with proton irradiation, which were 81.02%, 60.56% and 37.66%, respectively.

4 Discussion

We developed a new model, the “saturation model”, to overcome some limitations of the LQ model when applied to the context of lymphocyte radiosensitivity and to adapt to new radiobiological endpoints other than classical colony-forming assays. The LQ model, developed by Douglas Lea in 1962 [7], has been a foundational concept in radiation biology. This study has provided valuable insights into the dose–response relationship in various cell lines, particularly for chromosomal aberrations and SF2. However, new radiobiological endpoints have arisen, particularly based on apoptosis testing in lymphocytes. Given the heterogeneity in *in vitro* irradiation conditions (including dose, dose rate, and analysis time after irradiation) observed across studies evaluating correlations between radiation-induced lymphocyte apoptosis and effects on normal tissues [6], accurate models are needed to describe lymphocyte radiosensitivity. Nakamura in 1990 examined the radiosensitivity of dividing T-CD4+, T-CD8+ and total blood lymphocytes using colony formation assays and observed cell survival patterns consistent with the linear-quadratic dose–response model [14,17]. In contrast, most recent studies use other biological assays, where response curves typically have a saturated response at higher doses after an exponential trend [14].

Based on data from the literature, we introduced the concept of a saturation model, which assumes a negative exponential relationship between radiation dose and cell survival, following a Poisson distribution of DNA damage. This model addresses the inherent radiosensitivity of lymphocytes and the non-linearity of the dose–response relationship at high doses. Saturation of the lymphocyte response at higher doses was previously mentioned [14]. Our findings demonstrate that the saturation model exhibits superior performance compared to the conventional LQ model and its variants. This not only results in a lower residual error but also results in an insignificant correlation between the residual and the predicted value. The traditional LQ model is based on the assumption of a linear relationship between the energy delivered by radiation doses and the balance between unrepaired and repaired DNA damage [9]. Lymphoid and hematopoietic cells, such as lymphocytes, are known to exhibit high radiosensitivity, predominantly due to unrepaired DNA damage [14,35]. Conventionally, this radiosensitivity in lymphocytes was modeled using a linear approach [14,17]. However, the literature data indicate a nonlinear dose–response curve for lymphocytes at high radiation doses. This observation can be attributed to saturation of the response and subsequent DNA damage with increasing dose. Another possible mechanistic explanation for saturation could be the subset of radioresistant cells [39]. Based on Chinese hamster ovary cell lines subjected to gamma irradiation [40,41], some researchers have hypothesized that a resistant lymphocyte subpopulation dominates non-apoptotic cells or clonogenic survival. Other studies have indicated that lymphocyte subpopulations are heterogeneous, with varying levels of radiosensitivity [14]. For example, stimulated lymphocyte subpopulations displayed some radioresistance, with proportions of apoptotic cells remaining above 80% [20]. Radioresistance could be attributed to mixed lymphocyte populations of both unstimulated and stimulated cells in mammalian blood [42], leading to a saturation effect, as described by the saturation model [20]. In addition, some cancer cell lines exhibit a saturation effect under carbon ion irradiation, as evidenced by the negative beta value when fitted with the LQ model [39,43,44]. This observation suggests the potential applicability of the saturation model to cell lineages other than lymphocytes.

Indeed, several modifications to the LQ model have aimed at better aligning with observations in lymphocytes. One such adaptation involves incorporating an additional term into the LQ model proportional to the cube of the dose and signed opposite to both the linear and quadratic terms (known as the LQC model) [18]. However, our findings suggest that the LQC model less adequately captures the radiosensitivity of lymphocytes than does the saturation model. Although the LQ and LQC models can sometimes perform comparably to the SM, they often result in negative parameter estimates, which are inappropriate given their mechanistic interpretations. Additionally, these models are fundamentally empirical and based on polynomial functions, making extrapolation beyond the observed dose range inappropriate and potentially leading to unrealistic predictions. Beyond empirical approaches, various models, ranging from semi-mechanistic to fully mechanistic, have been developed to focus on DNA repair processes under irradiation, such as the RMR model. These models were evaluated based on the observation that survival plots at high doses deviate from the LQ model [45]. It has been proposed that a

kinetic model, such as the lethal–potentially lethal (LPL) model [46], may offer a more accurate representation of the response to large fractions or acute doses ranging from 15–24 Gy [45]. None of these models have effectively accounted for the rapid depletion and subsequent saturation state of lymphocyte survival at higher doses. Our results indicated that the application of the RMR model is not suitable for the lymphocyte dataset, as the estimation of the epsilon parameter is typically not significantly different from zero. This suggests that the model approximates a linear model.

The incorporation of the immune system into oncological treatments has highlighted the necessity of accurately modeling how treatments such as radiotherapy impact lymphocytes. A critical component of these models is the assumption of how lymphocytes respond to irradiation, which traditionally follows a linear dose–response relationship [10,47]. The saturation model, in place of the linear model, could enhance the precision of these onco-immunological models. The saturation model seems to better capture lymphocyte radiosensitivity patterns. However, in clinical settings, radiation is often administered in fractionated doses of typically approximately 2 Gy, which falls within the range where differences between the saturation and linear models seem small. The use of a saturation model rather than a linear model may be more relevant to higher or single doses and hypofractionation, such as 18 Gy for non-small cell lung cancer [48] or 25 Gy for hepatocellular carcinoma [49]. The distinction here lies in the saturation model's ability to more accurately reflect the biological response of lymphocytes under such conditions.

An interesting discovery was the greater residual errors at lower dose values, suggesting time-dependent variations in lymphocyte responses after irradiation. The saturation model revealed a negative linear relationship with time after irradiation, which underlines the potential utility of the saturation model in capturing time-dependent response variations. The observed time-dependent effect might be attributed to mitotic catastrophe, a phenomenon initiated by unrepaired DNA damage that prevents cells from successfully completing mitosis. The consequence of mitotic catastrophe is that the cell becomes senescent or dies through apoptosis or necrosis [50,51]. This theory aligns with our findings of a decrease in the survival rate over time at a rate of 0.009 per hour (0.9% reduction in survival rate per hour). Although this rate may seem negligible for enzymatic DNA repair processes, it has a significant effect on cell repopulation, approximating a doubling time of approximately $\ln(2)/0.009$ or 77 hours (approximately 3 days). This duration is consistent with the rapid turnover of lymphocytes (3–4 days), which expand in a lymphopenic environment *in vivo* [52].

Our research also investigated the influence of dose rate on lymphocyte survival. Low dose rates resulted in decreased lymphocyte survival during irradiation, with the inverse effect becoming evident immediately after irradiation. This finding implies that cell death is primarily induced by membrane damage rather than cell death due to DNA damage [38]. A study by Konings *et al.* demonstrated that at a sufficiently low dose rate of 0.006 Gy/min, lymphocyte survival linearly correlated with the dose rate [38]. These findings underline the complexity of lymphocyte responses to radiation and the importance of considering the temporal aspect. Similarly, a study by Nakamura *et al.* revealed that at sufficiently low doses (0–5 Gy) and prolonged incubation times post-irradiation (up to two weeks), the saturation model also approximates the LQ model for human lymphocyte radiosensitivity [17]. These observations align with our findings. Within the restricted dataset ranging from 0 to 5 Gy, there was no significant difference between the linear or saturation models. The LQ model without a beta component fitted with data from Nakamura *et al.* in 1990 was used as a lymphocyte radiosensitivity model to explain the *in vivo* RIL [53]. However, since RILs appear very early, within days following radiotherapy, assessing lymphocyte radiosensitivity early following irradiation is necessary. In such cases, the saturation model appeared to be more effective, which could also cover the circumstances in which the LQ model could be applied.

The introduced saturation model has potential for broader applications, including the exploration of differences in radiosensitivity between various lymphocyte subtypes or under different radiation conditions. The biological effect of proton beams is considered to be 10% greater than that of photon beams at the same radiation dose across multiple cancer cell lineages [54]. However, few studies have explored the differences in the radiosensitivity of peripheral blood lymphocytes under X-ray or proton irradiation *in vitro*. By applying the saturation model to the dataset of rodent splenic T-CD3+ lymphocyte survival, we revealed a greater cell-killing effect of protons than of X-rays. This observation aligns with previous research, which has suggested that X-rays and protons induce lymphocyte death through distinct mechanisms [25]. Protons, in particular, lead to relatively greater rates of cell death and necrosis when compared to X-rays [25]. Moreover, at the chromosomal level,

proton irradiation was shown to induce a greater rate of chromosomal aberrations than X-ray irradiation in human lymphocytes *in vitro* [55].

In addition, there was an association between radiation-induced apoptosis of T lymphocytes and a significantly lower risk of late-onset toxicity in patients treated with radiation in different tumor locations, especially tumors in the head and neck, uterine cervix, breast, and prostate [56]. This is the foundation of the RILA test. The current RILA test is based on the quantification of CD4 and CD8 T-cell apoptosis 48 hours after *in vitro* irradiation with 8 Gy; this is the condition that showed the most robust and reproducible results, with inter-individual variations far greater than the variations between samples from the same patient [56,57]. Evaluating a more precise radiosensitivity model for lymphocytes would allow further investigation of the correlation and association between lymphocytes at the *in vitro* level and patients at the *in vivo* level, such as in the case of RILA. For instance, the model allows investigation of the rate of lymphocyte reduction following irradiation or the saturation state the lymphocyte could reach for the survival rate at a high radiation dose and how these features correlate to the toxicity level of patients who underwent radiotherapy. Furthermore, radiosensitivity models were applied in other models as part of sub-models. For example, multiple types of immune-oncology models are affected by the impact of radiotherapy [47,58,59]. In these models, the linear model was applied to simulate the fraction of lymphocyte or T-CD8+ lymphocyte death induced by irradiation either in the tumor microenvironment or in the circulating blood. Since the linear model seems to overestimate the fraction of lymphocyte death at the high dose near the saturation level, the saturation model could be used as a substitution for a more accurate estimation.

5 Conclusion

The LQ model's limitations may be overcome in studying circulating lymphocyte radiosensitivity by a more suitable saturation model. The saturation model has potential applications in studying different types of lymphocytes and how they react to radiation and therefore could be applied to assays assessing interindividual radiosensitivity based on lymphocyte apoptosis, such as RILA.

Acknowledgments

This project has received financial support from the CNRS through the 80|Prime program, Ligue Contre le Cancer and French National Agency for Research 'Investissements d'Avenir' (n°ANR-10-EQPX1401) and Région Normandie (RIN CHOxTRaCC).

References

- [1] Ozsahin M, Crompton NEA, Gourgou S, Kramar A, Li L, Shi Y, et al. CD4 and CD8 T-Lymphocyte Apoptosis Can Predict Radiation-Induced Late Toxicity: A Prospective Study in 399 Patients. *Clinical Cancer Research* 2005;11:7426–33. <https://doi.org/10.1158/1078-0432.CCR-04-2634>.
- [2] Azria D, Riou O, Castan F, Nguyen TD, Peignaux K, Lemanski C, et al. Radiation-induced CD8 T-lymphocyte Apoptosis as a Predictor of Breast Fibrosis After Radiotherapy: Results of the Prospective Multicenter French Trial. *EBioMedicine* 2015;2:1965–73. <https://doi.org/10.1016/j.ebiom.2015.10.024>.
- [3] Brengues M, Lapierre A, Bourgier C, Pèlerin A, Özsahin M, Azria D. T lymphocytes to predict radiation-induced late effects in normal tissues. *Expert Review of Molecular Diagnostics* 2017;17:119–27. <https://doi.org/10.1080/14737159.2017.1271715>.
- [4] Mirjolet C, Merlin JL, Truc G, Noël G, Thariat J, Domont J, et al. RILA blood biomarker as a predictor of radiation-induced sarcoma in a matched cohort study. *EBioMedicine* 2019;41:420–6. <https://doi.org/10.1016/j.ebiom.2019.02.031>.
- [5] Fuentes-Raspall MJ, Caragol I, Alonso C, Ramón Y Cajal T, Fisas D, Seoane A, et al. Apoptosis for prediction of radiotherapy late toxicity: lymphocyte subset sensitivity and potential effect of TP53 Arg72Pro polymorphism. *Apoptosis* 2015;20:371–82. <https://doi.org/10.1007/s10495-014-1056-2>.

- [6] Fhoghlú MN, Barrett S. A Review of Radiation-Induced Lymphocyte Apoptosis as a Predictor of Late Toxicity After Breast Radiotherapy. *Journal of Medical Imaging and Radiation Sciences* 2019;50:337–44. <https://doi.org/10.1016/j.jmir.2019.02.004>.
- [7] Lea DE. *Actions of Radiations on Living Cells*. 2nd edition. Cambridge At The University Press; 1962.
- [8] Jones B, Dale R. The evolution of practical radiobiological modelling. *BJR* 2018;20180097. <https://doi.org/10.1259/bjr.20180097>.
- [9] McMahon SJ. The linear quadratic model: usage, interpretation and challenges. *Phys Med Biol* 2018;64:01TR01. <https://doi.org/10.1088/1361-6560/aaf26a>.
- [10] Jin J-Y, Mereniuk T, Yalamanchali A, Wang W, Machtay M, (Spring)Kong F-M, et al. A framework for modeling radiation induced lymphopenia in radiotherapy. *Radiotherapy and Oncology* 2020;144:105–13. <https://doi.org/10.1016/j.radonc.2019.11.014>.
- [11] McCullum L, Shin J, Xing S, Beekman C, Schuemann J, Hong T, et al. Predicting Severity of Radiation Induced Lymphopenia in Individual Proton Therapy Patients for Varying Dose Rate and Fractionation Using Dynamic 4-Dimensional Blood Flow Simulations. *International Journal of Radiation Oncology*Biophysics* 2023;116:1226–33. <https://doi.org/10.1016/j.ijrobp.2023.01.054>.
- [12] Chang DS, Lasley FD, Das IJ, Mendonca MS, Dynlacht JR. *Normal Tissue Radiation Response. Basic Radiotherapy Physics and Biology*, Cham: Springer International Publishing; 2021, p. 261–72. https://doi.org/10.1007/978-3-030-61899-5_25.
- [13] de Kermenguy F, Meziani L, Mondini M, Clémenson C, Morel D, Deutsch E, et al. Radio-induced lymphopenia in the era of anti-cancer immunotherapy. *International Review of Cell and Molecular Biology*, Elsevier; 2023, p. S1937644823000229. <https://doi.org/10.1016/bs.ircmb.2023.03.002>.
- [14] Paganetti H. A review on lymphocyte radiosensitivity and its impact on radiotherapy. *Front Oncol* 2023;13:1201500. <https://doi.org/10.3389/fonc.2023.1201500>.
- [15] Rohatgi A. *Webplotdigitizer: Version 4.6* 2022.
- [16] Bodgi L, Canet A, Pujo-Menjouet L, Lesne A, Victor J-M, Foray N. Mathematical models of radiation action on living cells: From the target theory to the modern approaches. A historical and critical review. *Journal of Theoretical Biology* 2016;394:93–101. <https://doi.org/10.1016/j.jtbi.2016.01.018>.
- [17] Nakamura N, Kusunoki Y, Akiyama M. Radiosensitivity of CD4 or CD8 positive human T-lymphocytes by an in vitro colony formation assay. *Radiat Res* 1990;123:224–7.
- [18] Joiner M, Kogel AJ van der, editors. *Basic clinical radiobiology*. 4. ed. London: Hodder Arnold; 2009.
- [19] Tobias CA. The repair-misrepair model in radiobiology: comparison to other models. *Radiat Res Suppl* 1985;8:S77-95.
- [20] Heylmann D, Badura J, Becker H, Fahrer J, Kaina B. Sensitivity of CD3/CD28-stimulated versus non-stimulated lymphocytes to ionizing radiation and genotoxic anticancer drugs: key role of ATM in the differential radiation response. *Cell Death Dis* 2018;9:1053. <https://doi.org/10.1038/s41419-018-1095-7>.
- [21] PlotDigitizer n.d. <https://plotdigitizer.com>.
- [22] Pinheiro J, Bates D, R Core Team. *nlme: Linear and Nonlinear Mixed Effects Models*. 2022.
- [23] *Mixed-Effects Models in S and S-PLUS*. New York: Springer-Verlag; 2000. <https://doi.org/10.1007/b98882>.

- [24] R Core Team. R: A Language and Environment for Statistical Computing. Vienna, Austria: R Foundation for Statistical Computing; 2021.
- [25] Miszczyk J, Rawojć K, Panek A, Borkowska A, Prasanna PGS, Ahmed MM, et al. Do protons and X-rays induce cell-killing in human peripheral blood lymphocytes by different mechanisms? *Clinical and Translational Radiation Oncology* 2018;9:23–9. <https://doi.org/10.1016/j.ctro.2018.01.004>.
- [26] Bordón E, Henríquez Hernández LA, Lara PC, Pinar B, Fontes F, Rodríguez Gallego C, et al. Prediction of clinical toxicity in localized cervical carcinoma by radio-induced apoptosis study in peripheral blood lymphocytes (PBLs). *Radiat Oncol* 2009;4:58. <https://doi.org/10.1186/1748-717X-4-58>.
- [27] Wilkins RC, Wilkinson D, Maharaj HP, Bellier PV, Cybulski MB, McLean JRN. Differential apoptotic response to ionizing radiation in subpopulations of human white blood cells. *Mutation Research/Genetic Toxicology and Environmental Mutagenesis* 2002;513:27–36. [https://doi.org/10.1016/S1383-5718\(01\)00290-X](https://doi.org/10.1016/S1383-5718(01)00290-X).
- [28] Horn S, Barnard S, Brady D, Prise KM, Rothkamm K. Combined Analysis of Gamma-H2AX/53BP1 Foci and Caspase Activation in Lymphocyte Subsets Detects Recent and More Remote Radiation Exposures. *Radiation Research* 2013;180:603–9. <https://doi.org/10.1667/RR13342.1>.
- [29] Torudd J, Protopopova M, Sarimov R, Nygren J, Eriksson S, Marková E, et al. Dose – response for radiation-induced apoptosis, residual 53BP1 foci and DNA-loop relaxation in human lymphocytes. *International Journal of Radiation Biology* 2005;81:125–38. <https://doi.org/10.1080/09553000500077211>.
- [30] Falcke S, Rühle P, Deloch L, Fietkau R, Frey B, Gaipl U. Clinically Relevant Radiation Exposure Differentially Impacts Forms of Cell Death in Human Cells of the Innate and Adaptive Immune System. *IJMS* 2018;19:3574. <https://doi.org/10.3390/ijms19113574>.
- [31] Benderitter M, Durand V, Caux C, Voisin P. Clearance of Radiation-Induced Apoptotic Lymphocytes: *Ex Vivo* Studies and an *In Vitro* Co-culture Model. *Radiation Research* 2002;158:464–74. [https://doi.org/10.1667/0033-7587\(2002\)158\[0464:CORIAL\]2.0.CO;2](https://doi.org/10.1667/0033-7587(2002)158[0464:CORIAL]2.0.CO;2).
- [32] Anderson RE, Sprent J, Miller JFAP. Radiosensitivity of T and B lymphocytes. I. Effect of irradiation on cell migration. *Eur J Immunol* 1974;4:199–203. <https://doi.org/10.1002/eji.1830040309>.
- [33] Heylmann D, Ponath V, Kindler T, Kaina B. Comparison of DNA repair and radiosensitivity of different blood cell populations. *Sci Rep* 2021;11:2478. <https://doi.org/10.1038/s41598-021-81058-1>.
- [34] Pugh JL, Sukhina AS, Seed TM, Manley NR, Sempowski GD, Van Den Brink MRM, et al. Histone Deacetylation Critically Determines T Cell Subset Radiosensitivity. *The Journal of Immunology* 2014;193:1451–8. <https://doi.org/10.4049/jimmunol.1400434>.
- [35] Radford IR. Radiation Response of Mouse Lymphoid and Myeloid Cell Lines. Part I. Sensitivity to Killing by Ionizing Radiation, Rate of Loss of Viability, and Cell Type of Origin. *International Journal of Radiation Biology* 1994;65:203–15. <https://doi.org/10.1080/09553009414550241>.
- [36] Prosser JS. Survival of Human T and B Lymphocytes after X-irradiation. *International Journal of Radiation Biology and Related Studies in Physics, Chemistry and Medicine* 1976;30:459–65. <https://doi.org/10.1080/09553007614551271>.
- [37] Schmitz A, Bayer J, Déchamps N, Thomas G. Intrinsic susceptibility to radiation-induced apoptosis of human lymphocyte subpopulations. *International Journal of Radiation Oncology* Biology* Physics* 2003;57:769–78. [https://doi.org/10.1016/S0360-3016\(03\)00637-0](https://doi.org/10.1016/S0360-3016(03)00637-0).
- [38] Konings AWT. Dose-rate effects on lymphocyte survival. *JRR* 1981;22:282–5. <https://doi.org/10.1269/jrr.22.282>.

- [39] K. Weyrather, S. Ritter, M. Scholz, W. RBE for carbon track-segment irradiation in cell lines of differing repair capacity. *International Journal of Radiation Biology* 1999;75:1357–64. <https://doi.org/10.1080/095530099139232>.
- [40] Denekamp J, Whitmore GF, Jeggo P. Biphasic Survival Curves for XRS Radiosensitive Cells: Subpopulations or Transient Expression of Repair Competence? *International Journal of Radiation Biology* 1989;55:605–17. <https://doi.org/10.1080/09553008914550651>.
- [41] Jeggo PA. X-ray sensitive mutants of Chinese hamster ovary cell line: radio-sensitivity of DNA synthesis. *Mutation Research/DNA Repair Reports* 1985;145:171–6. [https://doi.org/10.1016/0167-8817\(85\)90024-0](https://doi.org/10.1016/0167-8817(85)90024-0).
- [42] Pham T-N, Coupey J, Candeias SM, Ivanova V, Valable S, Thariat J. Beyond lymphopenia, unraveling radiation-induced leucocyte subpopulation kinetics and mechanisms through modeling approaches. *J Exp Clin Cancer Res* 2023;42:50. <https://doi.org/10.1186/s13046-023-02621-4>.
- [43] Yagi M, Takahashi Y, Minami K, Matsuura T, Nam J-M, Onodera Y, et al. A Consistent Protocol Reveals a Large Heterogeneity in the Biological Effectiveness of Proton and Carbon-Ion Beams for Various Sarcoma and Normal-Tissue-Derived Cell Lines. *Cancers* 2022;14:2009. <https://doi.org/10.3390/cancers14082009>.
- [44] Habermehl D, Ilicic K, Dehne S, Rieken S, Orschiedt L, Brons S, et al. The Relative Biological Effectiveness for Carbon and Oxygen Ion Beams Using the Raster-Scanning Technique in Hepatocellular Carcinoma Cell Lines. *PLoS ONE* 2014;9:e113591. <https://doi.org/10.1371/journal.pone.0113591>.
- [45] Scheidegger S, Fuchs HU, Zaugg K, Bodis S, Fuchsli RM. Using State Variables to Model the Response of Tumour Cells to Radiation and Heat: A Novel Multi-Hit-Repair Approach. *Computational and Mathematical Methods in Medicine* 2013;2013:1–15. <https://doi.org/10.1155/2013/587543>.
- [46] Curtis SB. Lethal and potentially lethal lesions induced by radiation--a unified repair model. *Radiat Res* 1986;106:252–70.
- [47] Sung W, Grassberger C, McNamara AL, Basler L, Ehrbar S, Tanadini-Lang S, et al. A tumor-immune interaction model for hepatocellular carcinoma based on measured lymphocyte counts in patients undergoing radiotherapy. *Radiotherapy and Oncology* 2020;151:73–81. <https://doi.org/10.1016/j.radonc.2020.07.025>.
- [48] Iocolano M, Wild AT, Hannum M, Zhang Z, Simone CB, Gelblum D, et al. Hypofractionated vs. conventional radiation therapy for stage III non-small cell lung cancer treated without chemotherapy. *Acta Oncologica* 2020;59:164–70. <https://doi.org/10.1080/0284186X.2019.1675907>.
- [49] Scorsetti M, Comito T, Cozzi L, Clerici E, Tozzi A, Franzese C, et al. The challenge of inoperable hepatocellular carcinoma (HCC): results of a single-institutional experience on stereotactic body radiation therapy (SBRT). *J Cancer Res Clin Oncol* 2015;141:1301–9. <https://doi.org/10.1007/s00432-015-1929-y>.
- [50] Adjemian S, Oltean T, Martens S, Wiernicki B, Goossens V, Vanden Berghe T, et al. Ionizing radiation results in a mixture of cellular outcomes including mitotic catastrophe, senescence, methuosis, and iron-dependent cell death. *Cell Death Dis* 2020;11:1003. <https://doi.org/10.1038/s41419-020-03209-y>.
- [51] Vakifahmetoglu H, Olsson M, Zhivotovsky B. Death through a tragedy: mitotic catastrophe. *Cell Death Differ* 2008;15:1153–62. <https://doi.org/10.1038/cdd.2008.47>.
- [52] Asquith B, Debacq C, Macallan DC, Willems L, Bangham CRM. Lymphocyte kinetics: the interpretation of labelling data. *Trends in Immunology* 2002;23:596–601. [https://doi.org/10.1016/S1471-4906\(02\)02337-2](https://doi.org/10.1016/S1471-4906(02)02337-2).
- [53] Kim Y, Choe B-Y, Suh TS, Sung W. A Mathematical Model for Predicting Patient Responses to Combined Radiotherapy with CTLA-4 Immune Checkpoint Inhibitors. *Cells* 2023;12:1305. <https://doi.org/10.3390/cells12091305>.

- [54] Girdhani S, Sachs R, Hlatky L. Biological Effects of Proton Radiation: What We Know and Don't Know. *Radiation Research* 2013;179:257–72. <https://doi.org/10.1667/RR2839.1>.
- [55] Todorov SL, Grigor'ev YuG, Rizhov NI, Ivanov BA, Malyutina TS, Mileva MS. Dose-response relationship for chromosome aberrations induced by X-rays or 50 MeV protons in human peripheral lymphocytes. *Mutation Research/Fundamental and Molecular Mechanisms of Mutagenesis* 1972;15:215–20. [https://doi.org/10.1016/0027-5107\(72\)90035-8](https://doi.org/10.1016/0027-5107(72)90035-8).
- [56] Lapierre A, Gourgou S, Brengues M, Quéro L, Deutsch É, Milliat F, et al. Tumour and normal tissue radiosensitivity. *Cancer/Radiothérapie* 2022;26:96–103. <https://doi.org/10.1016/j.canrad.2021.11.008>.
- [57] Ozsahin M, Ozsahin H, Shi Y, Larsson B, Würzler FE, Crompton NEA. Rapid assay of intrinsic radiosensitivity based on apoptosis in human CD4 and CD8 T-lymphocytes. *International Journal of Radiation Oncology*Biophysics* 1997;38:429–40. [https://doi.org/10.1016/S0360-3016\(97\)00038-2](https://doi.org/10.1016/S0360-3016(97)00038-2).
- [58] Sung W, Cho B. Modeling of radiation effects to immune system: a review. *J Korean Phys Soc* 2022;81:1013–9. <https://doi.org/10.1007/s40042-022-00574-z>.
- [59] Anderson HG, Takacs GP, Harris DC, Kuang Y, Harrison JK, Stepien TL. Global stability and parameter analysis reinforce therapeutic targets of PD-L1-PD-1 and MDSCs for glioblastoma. *J Math Biol* 2024;88:10. <https://doi.org/10.1007/s00285-023-02027-y>.

Figure captions

Figure 1. Literature selection strategy flowchart.

Legend: To ensure consistency in model evaluation, quantitative methods other than annexin V assays or focused on species other than human lymphocytes were excluded.

Figure 2. Effect of different parameters (dose, time following irradiation, and dose rate) on lymphocyte radiosensitivity (A) Fraction of radiation-induced lymphocyte apoptosis by dose according to previous studies [25,26,28,29,31]; (B) Fraction of radiation-induced lymphocyte apoptosis by time after irradiation according to previous studies [25,26,28,29,31]. (C) Effect of dose rate on bovine lymphocyte survival immediately after irradiation; (D) effect of dose immediately after irradiation at 0.006 Gy/min

Legend: The size of the dot in figure A represents the incubation time after *in vitro* irradiation in each study. The size of the dot in figure B represents the dose applied in each study. For both figures A and B, the dots represent the data extracted from the literature and the curve was fitted with the data using locally estimated scatterplot smoothing to represent the data trend. The different colors represent data from different publications.

Figure 3. (A) Model fitting of the linear model, linear quadratic (LQ) model, linear-quadratic-cubic (LQC) model, repair-misrepair (RMR) model, and saturation model with the data of human peripheral blood lymphocytes by radiation dose. (B) Residual versus fitted values for the linear model (B.1), LQ model (B.2), LQC model (B.3), RMR model (B.4), and saturation model (B.5)

Legend: For panel A, the dot represents the data extracted from the literature; the size of the dot represents the incubation time after *in vitro* irradiation in each study; and the curve represents the model fit of the data with either a linear model (blue), linear quadratic model (yellow), linear-quadratic-cubic model (gray), repair-misrepair model (red) or saturation model (light blue). In panel B, R represents the Pearson correlation coefficient of the fitted and residual values.

Figure 4. Model fitting of the saturation model with the data with distinct estimates of the saturated survival rate (SF_{sat}) according to different incubation time post-irradiation. (A) Model fitting of the saturation model with the data stratified by time after irradiation; (B) residual versus fitted value, with Pearson correlation coefficient R; and (C) linear relationship between the saturated survival rate (SF_{sat}) and incubation time post-irradiation.

Legend: For figure A, dots represent the literature data; the curve represents the model fitting of the data with the saturation model, and the different colors represent different incubation times after *in vitro* irradiation: 4 hours (blue), 24 hours (yellow), 48 hours (gray), and 72 hours (red). For figure B, R represents the Pearson correlation coefficient of the fitted and residual values.

Figure 5. Saturation model (A) and linear model (B) with post-irradiation time effect on model parameters. (A.1, B.1) Model fitting of the saturation model (A.1) or linear model (B.1) with the total dataset stratified by time after irradiation; (A.2, B.2) Model fitting of the saturation model (A.2) or linear model (B.2) with the restricted dataset where the dose did not exceed 5 Gy stratified by time after irradiation.

Legend: The dots represent the data extracted from the literature; the curve represents the model fitting of the data with the saturation model, and the different colors represent different incubation times after *in vitro* irradiation: 4 hours (blue), 24 hours (yellow), 48 hours (gray), and 72 hours (red).

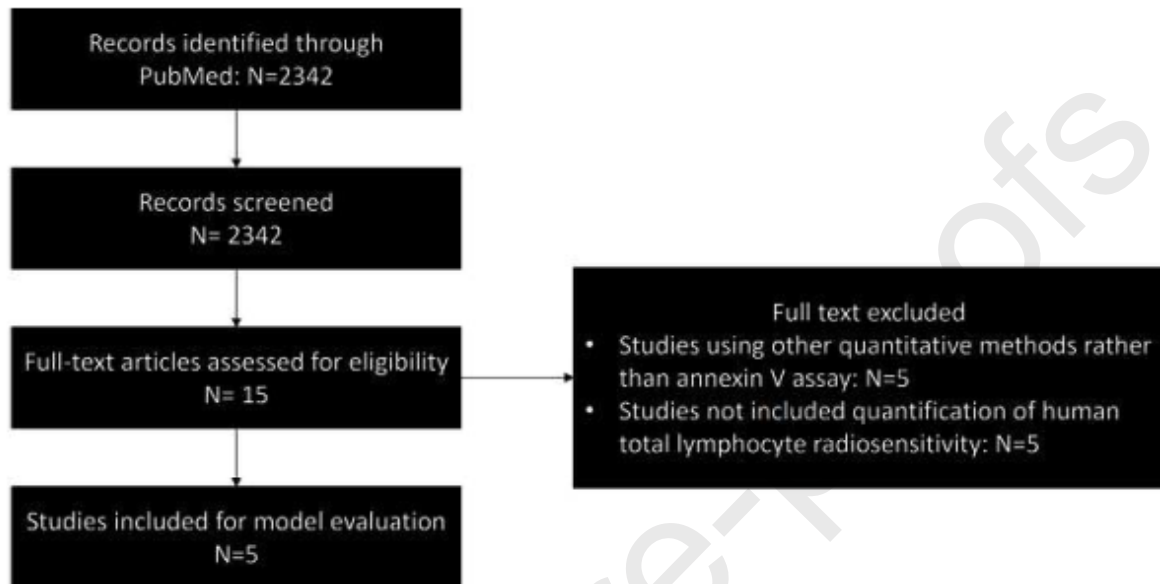
Figure 6. Application of the saturation model to (A, B) human lymphocytes extracted from Heylmann *et al.* 2018 [20], which included peripheral blood lymphocytes, helper T lymphocytes, cytotoxic T lymphocytes, and lymphocyte progenitor cells. The cells were either left unstimulated (A) or stimulated (B) with CD3/CD28 antibodies. (C) rodent splenic T-CD8+ lymphocyte survival data stratified by time and radiation dose under either X-ray or proton irradiation using a saturation model (C.1) or linear model (C.2).

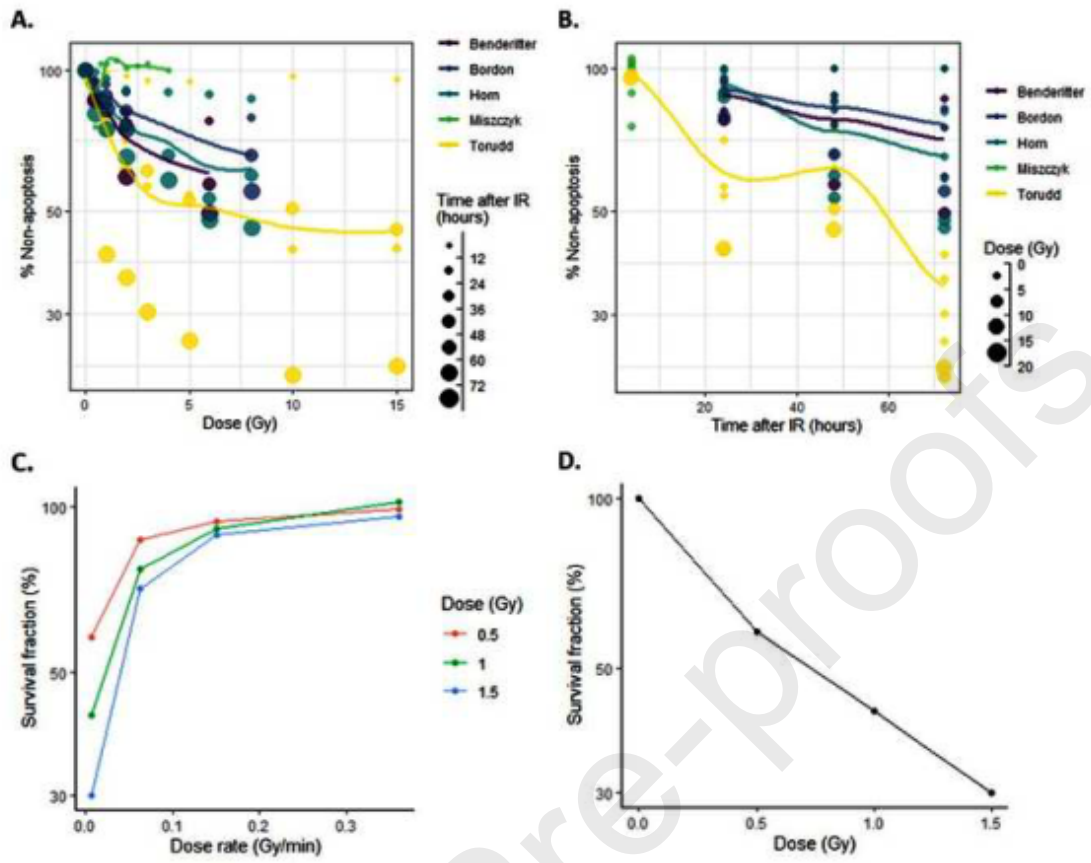
Legend: Dots represent our original data; the curve represents the model fitting of the data with the models. For panels A and B, different colors in the curves represent different models, including the linear model (blue), linear-

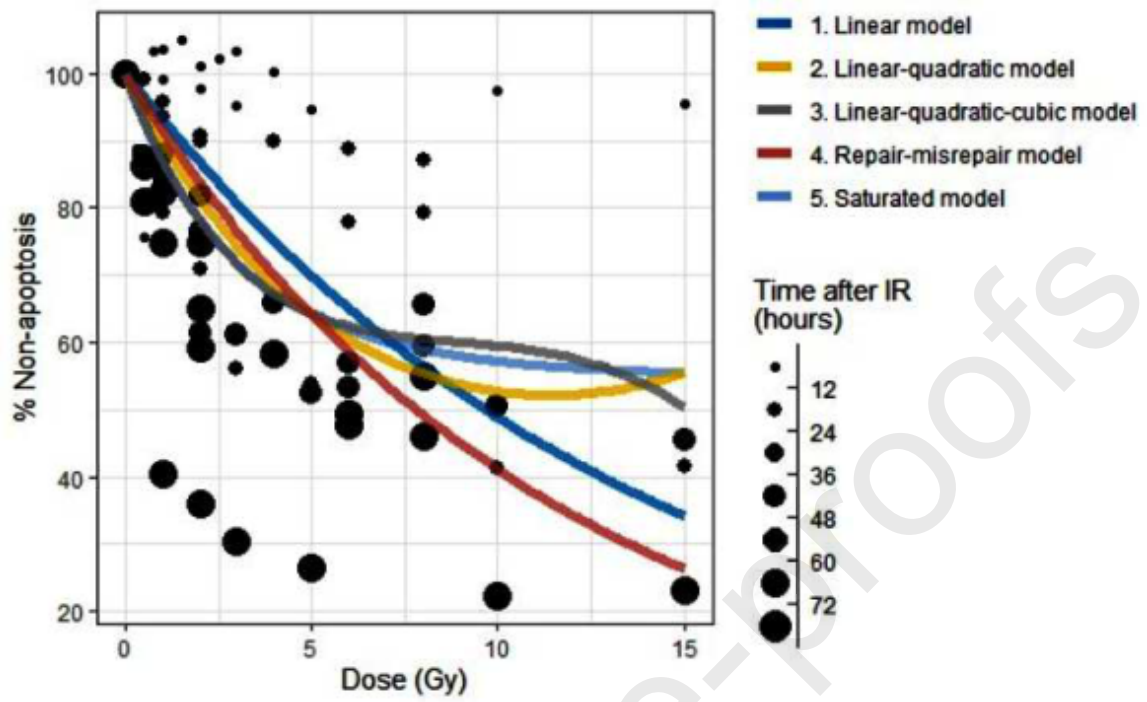
quadratic model (yellow), linear-quadratic-cubic model (gray), repair-misrepair model (red), and saturation model (light blue). In panel C, the different colors represent different incubation times after *in vitro* irradiation: 24 hours

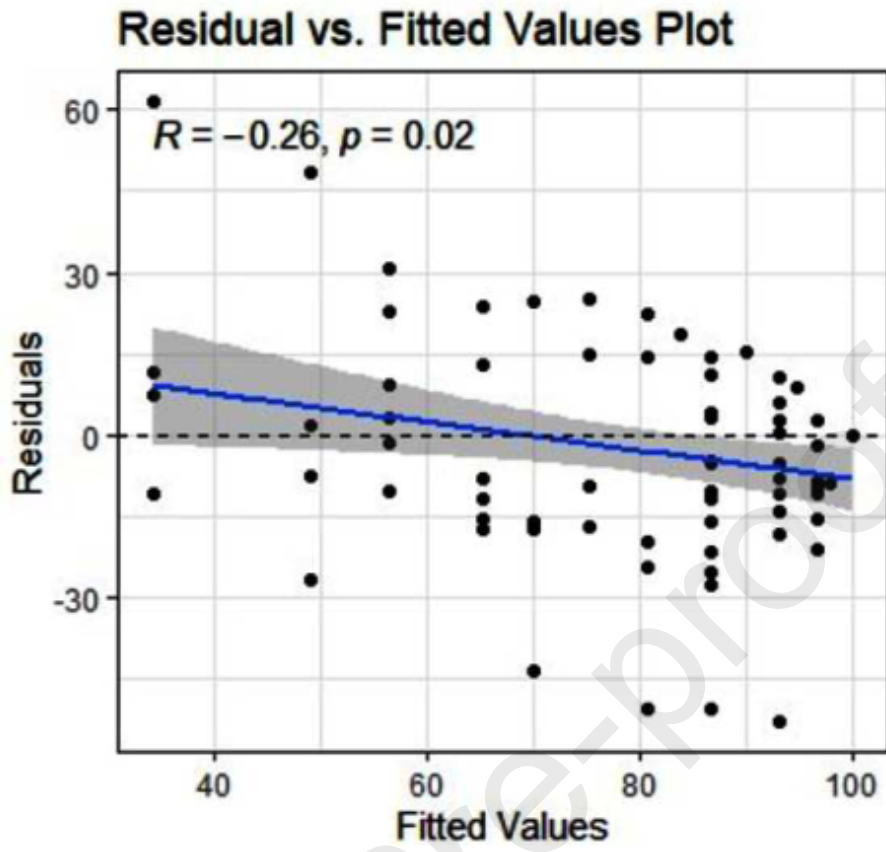
Figure 1

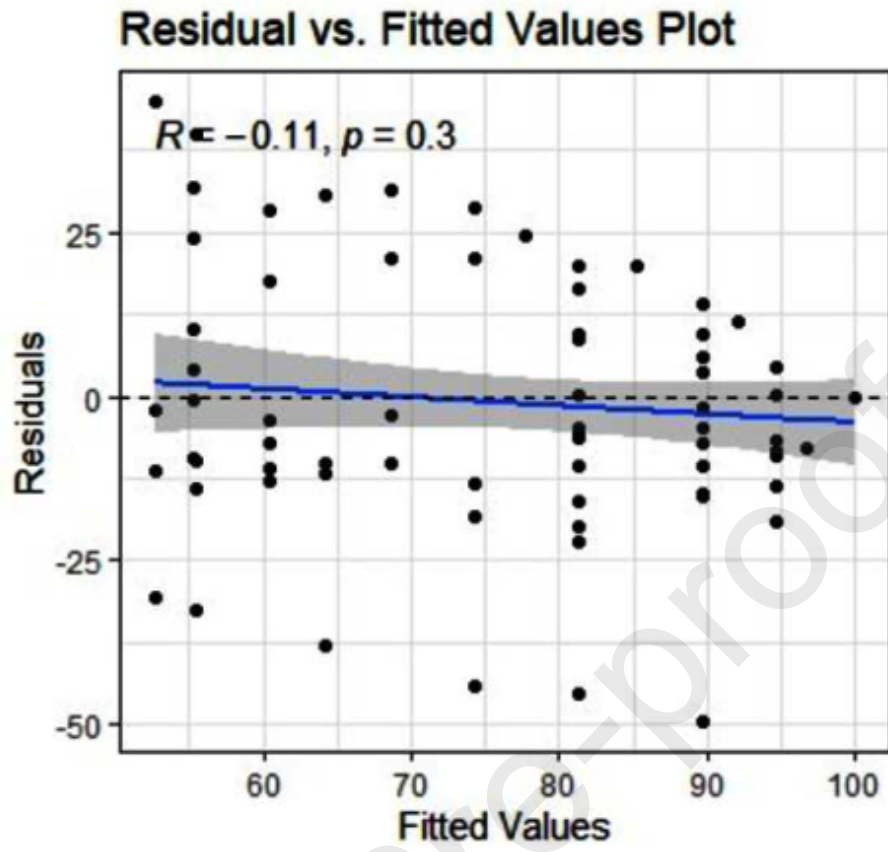
[Click here to access/download;Figure;Figure1.jpg](#)

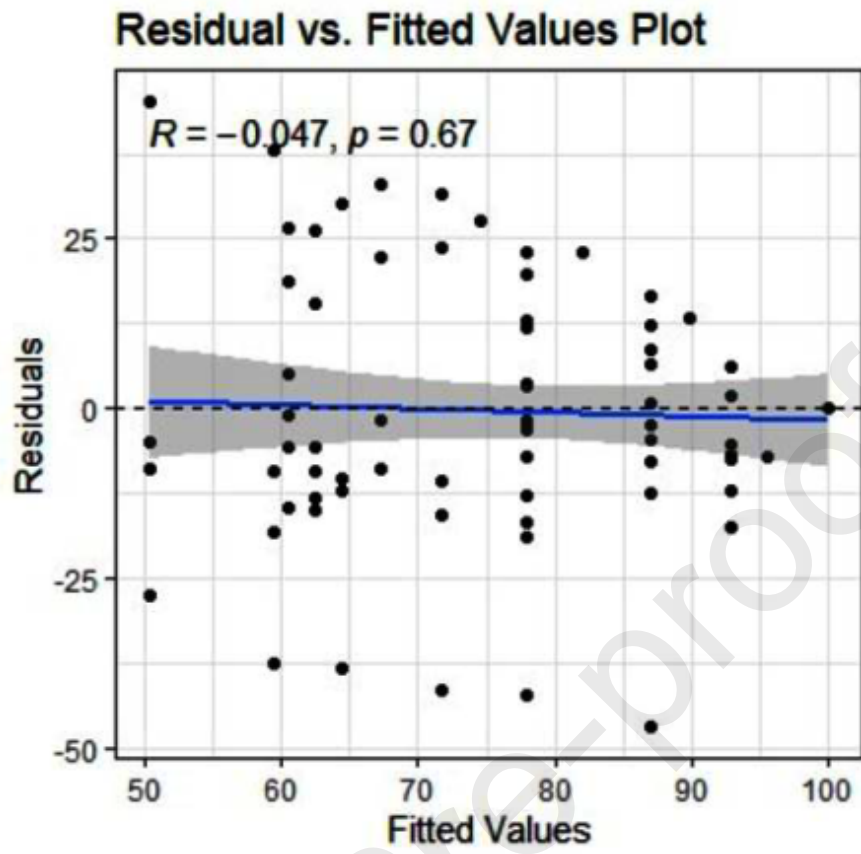


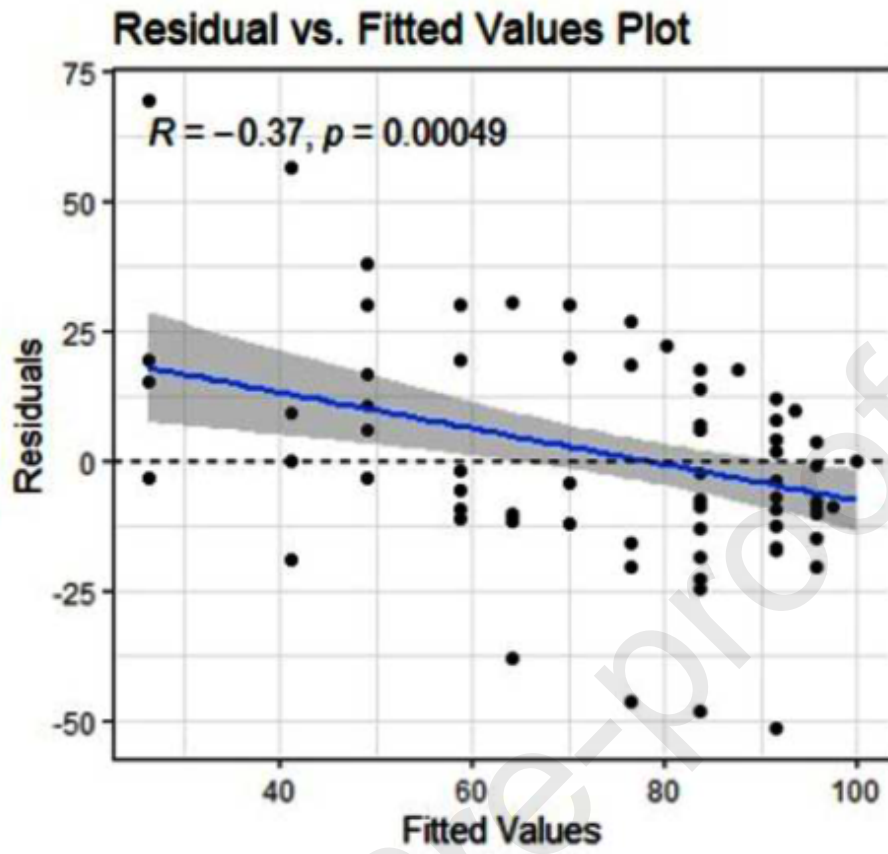


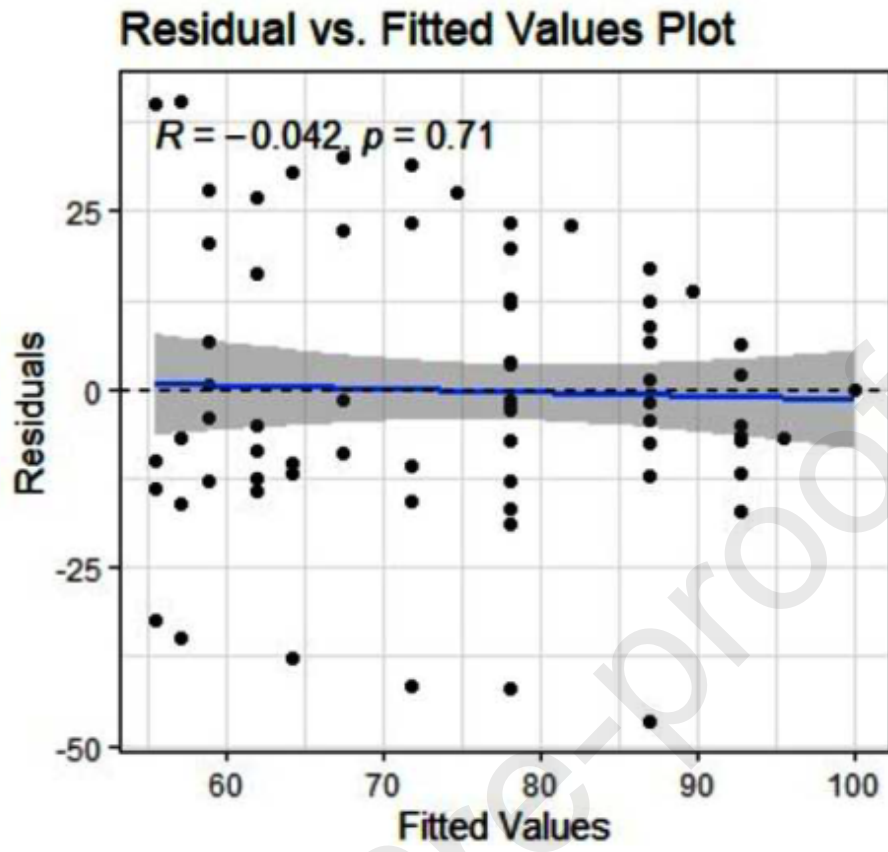


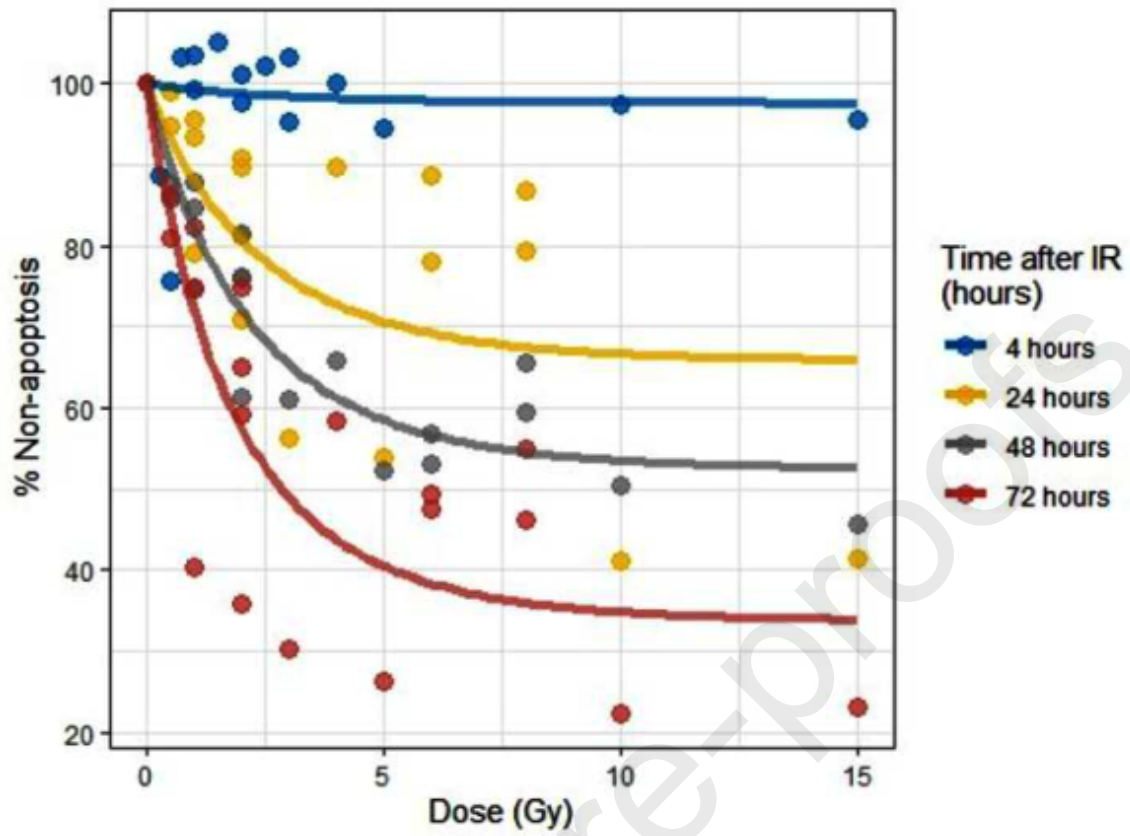


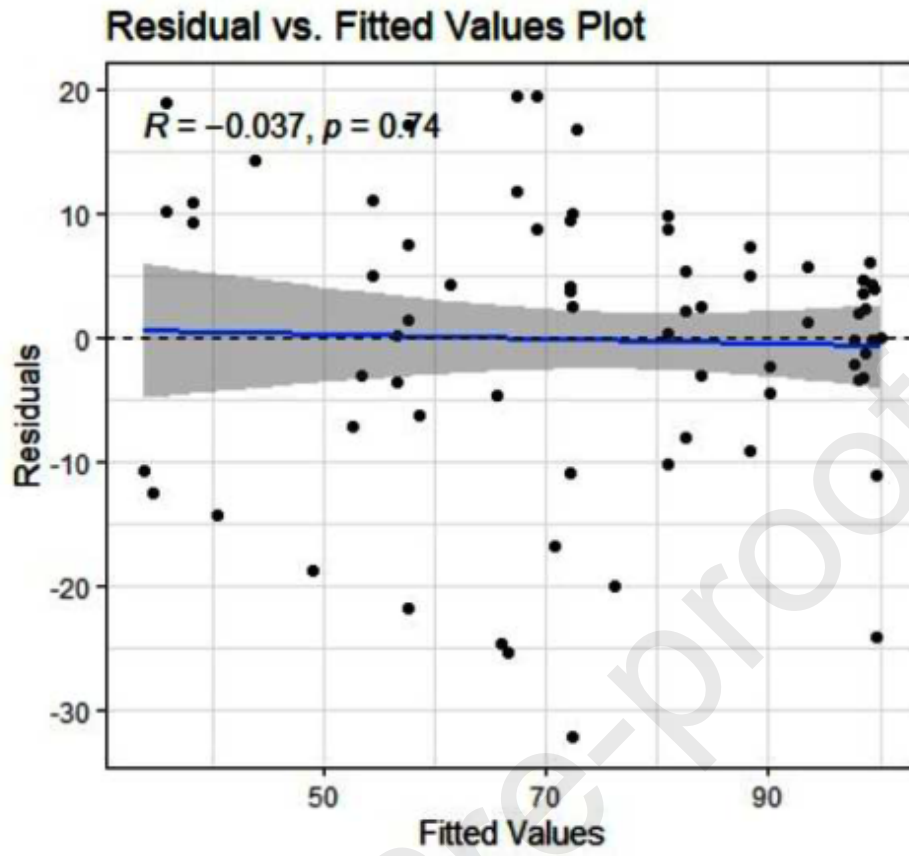


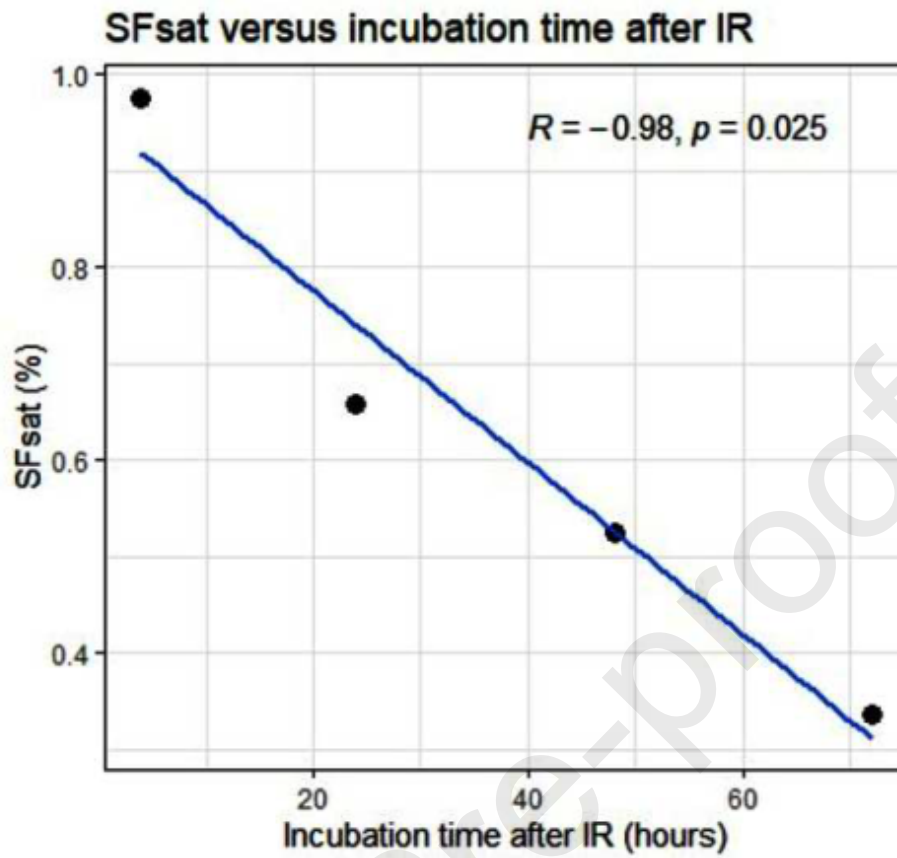


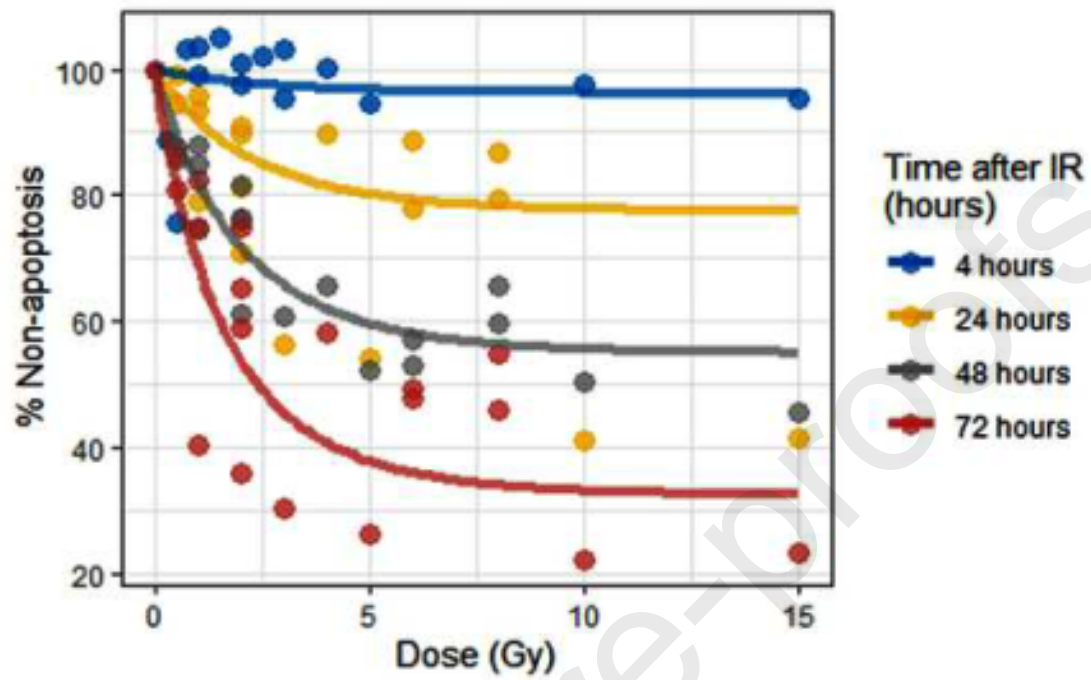




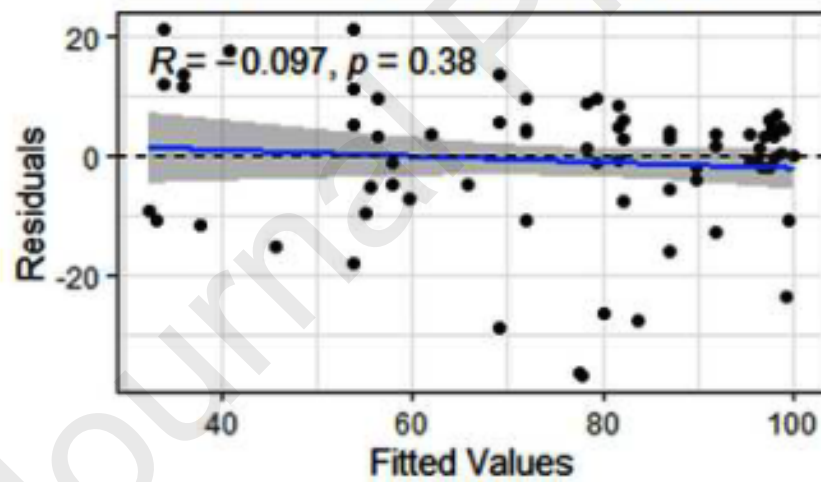


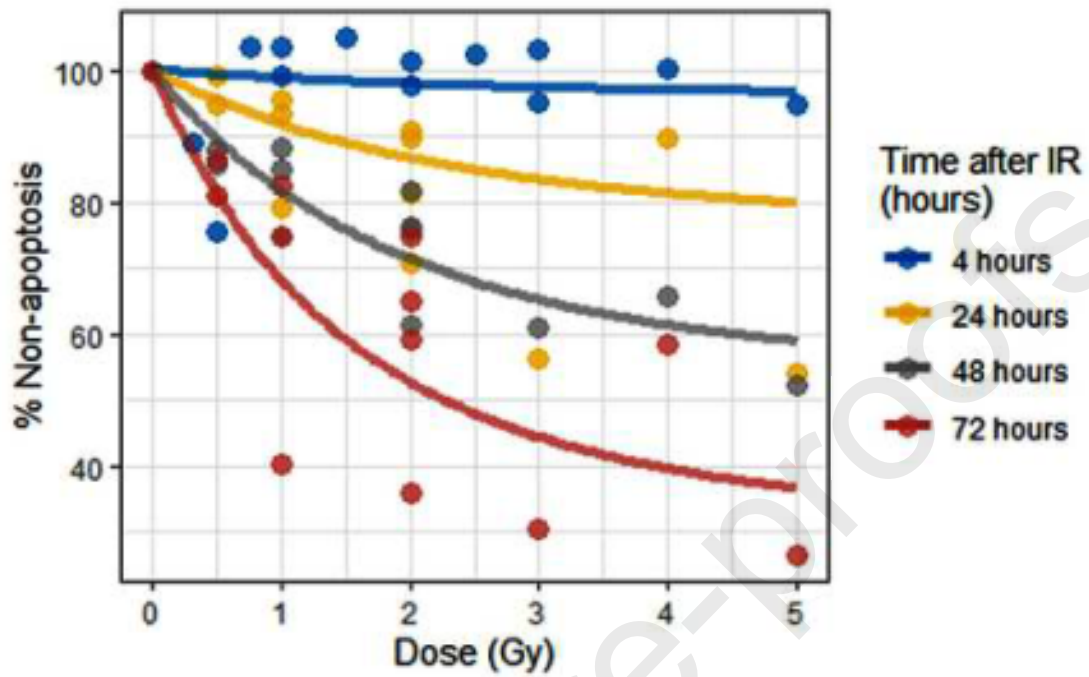




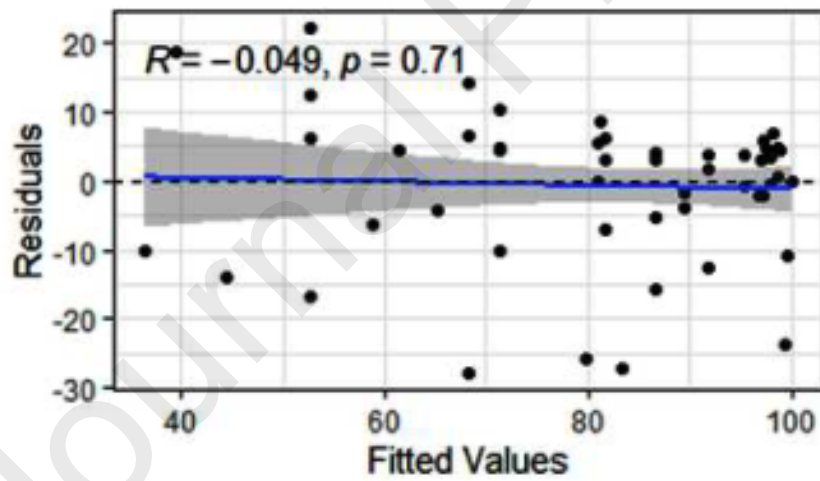


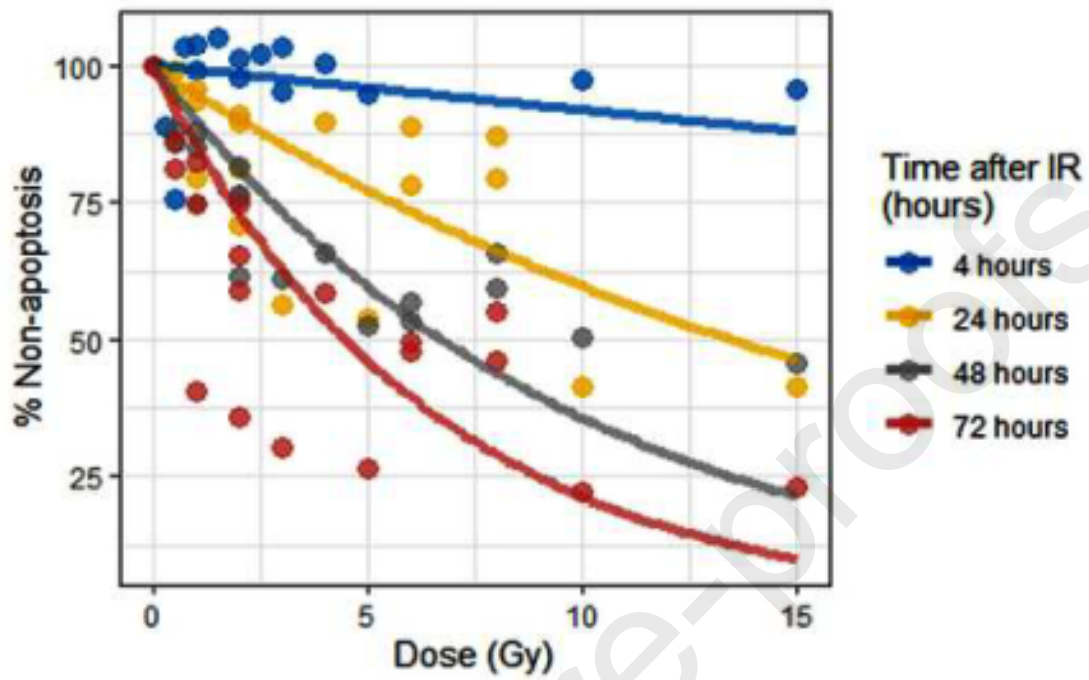
Residual vs. Fitted Values Plot



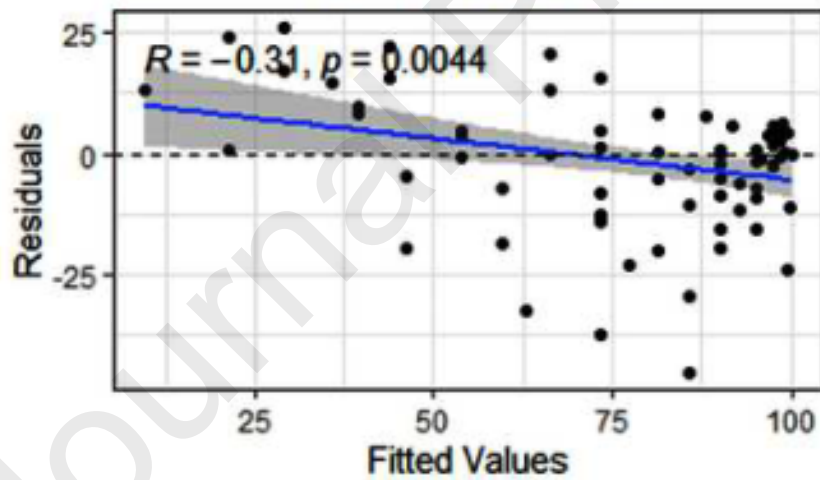


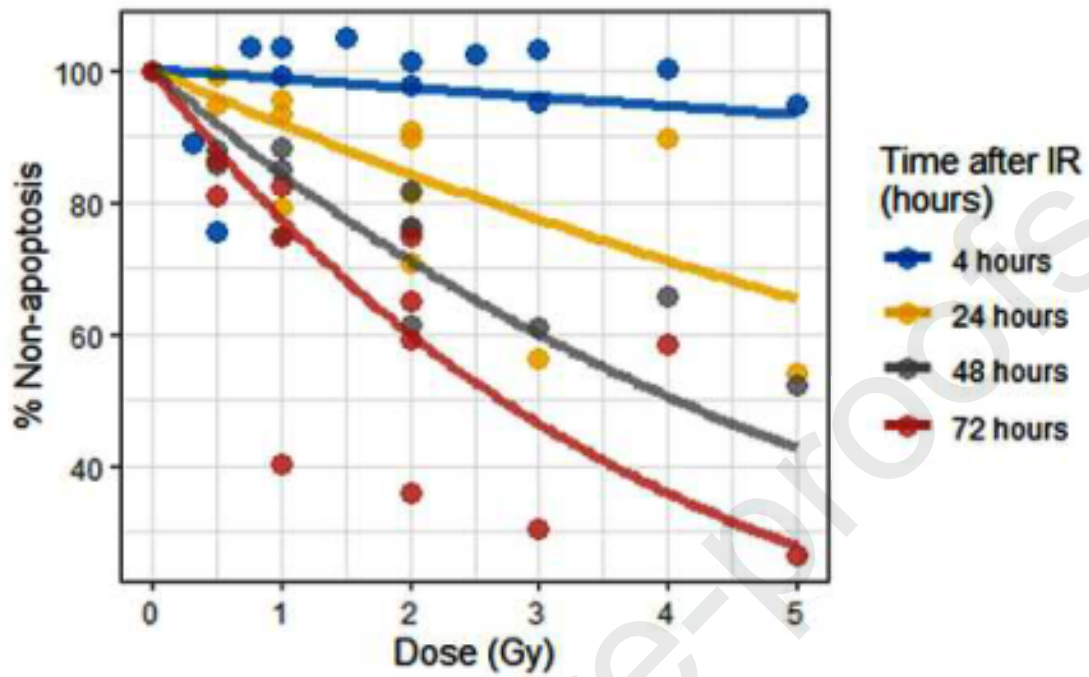
Residual vs. Fitted Values Plot



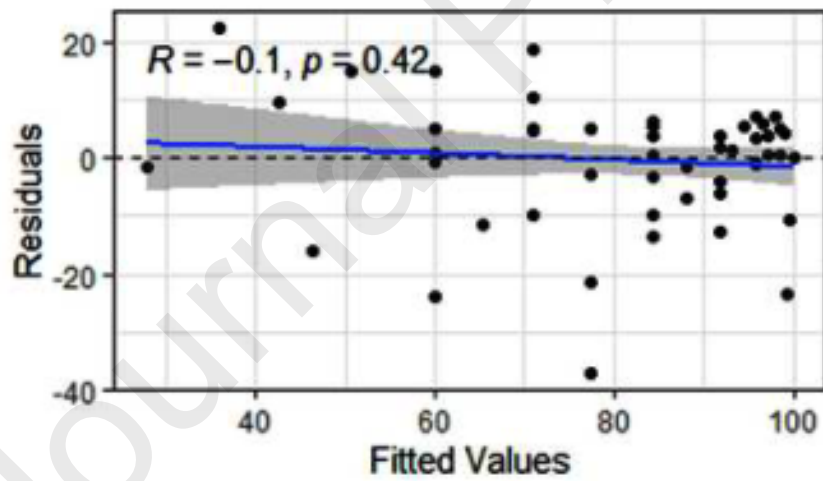


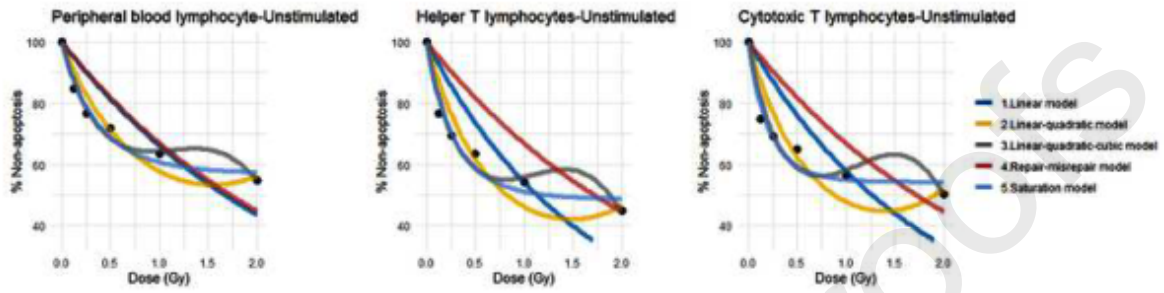
Residual vs. Fitted Values Plot

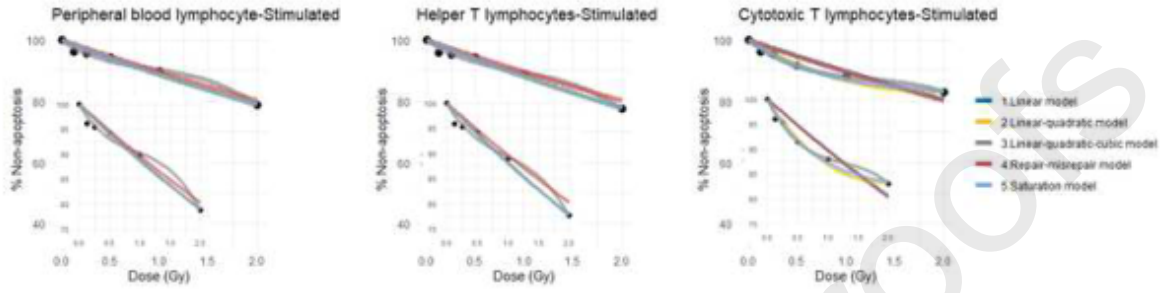


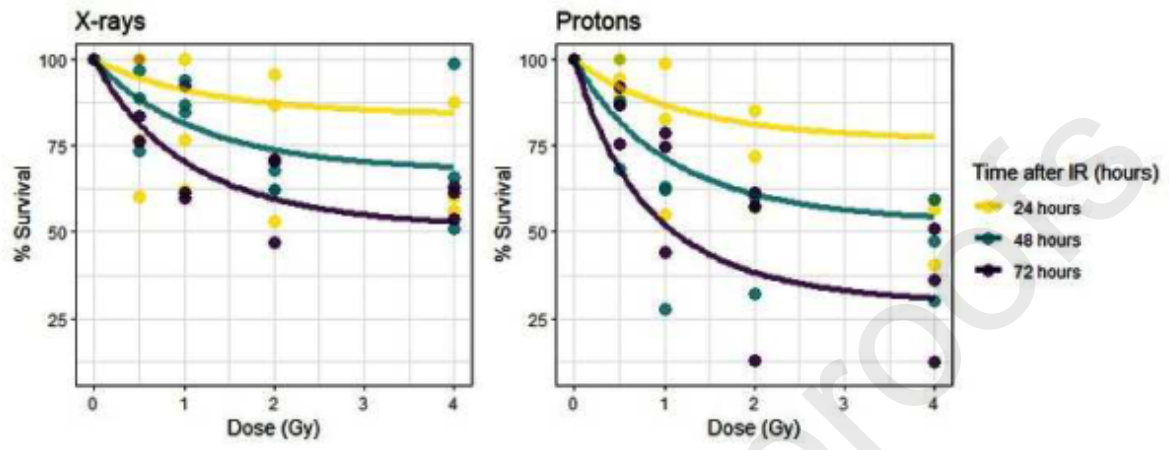


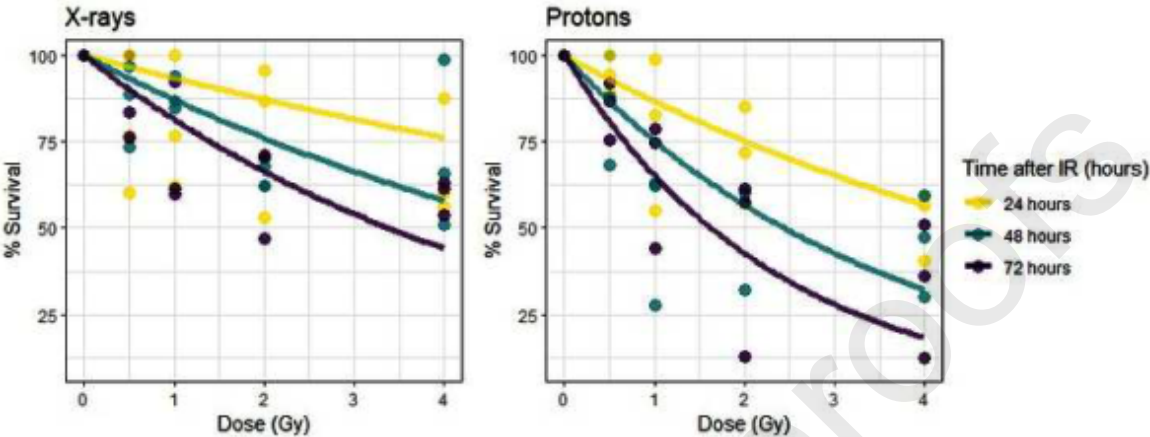
Residual vs. Fitted Values Plot











Journal Pre-proof